Electronic Structure of Strained Silicon- and Sulfur-Bridged [1]Ferrocenophanes and an Analogous Dicarbon-Bridged [2]Ferrocenophane: An Investigation by Photoelectron Spectroscopy and Density-Functional Theory

Stephen Barlow, Mark J. Drewitt, Tessa Dijkstra, Jennifer C. Green,*
Dermot O'Hare, Conrad Whittingham, and Hamish H. Wynn

*Inorganic Chemistry Laboratory, University of Oxford, South Parks Road,
Oxford OX1 3QR, U.K.*

Derek P. Gates, Ian Manners, James M. Nelson, and John K. Pudelski

*Department of Chemistry, University of Toronto, 80 St. George Street,
Toronto M5S 3H6, Ontario, Canada*

He I and He II photoelectron (PE) spectra of $[Fe(\eta\text{-}C_5H_4)_2SiMe_2]$ (**1**), $[Fe(\eta\text{-}C_5H_3Me)_2SiMe_2]$ (**2**), $[Fe(\eta\text{-}C_5H_4)(\eta\text{-}C_5Me_4)SiMe_2]$ (**3**), $[Fe(\eta\text{-}C_5Me_4)_2SiMe_2]$ (**4**), $[Fe(\eta\text{-}C_5H_4)_2C_2H_4]$ (**5**), and $[Fe(\eta\text{-}C_5H_4)_2S]$ (**6**) have been measured and assigned. The d bands of **1**−**5** show less structure than that of ferrocene, consistent with a loss of degeneracy of the e_2 orbitals on bending. Compound **6**, which has the largest inter-ring angle of the series, shows two separate d bands. The trend in the first ionization energy closely parallels the variation in oxidation potential. Density functional calculations on **1**, **5**, and **6** give geometries in good agreement with the structures found from X-ray diffraction. Ionization energies calculated were also in excellent agreement with experiment. Good agreement was also found between the calculated d−d transitions and the position of the first spin-allowed band in the optical spectra of **1** and **6**. Estimates of strain energy in bending ferrocene and octamethylferrocene were obtained, and octamethylferrocene was shown to be significantly more difficult to bend. Compounds **1** and **6** were both shown to have a low-lying empty orbital, partially located on the *ipso* carbon, which is a possible site for nucleophilic attack in the polymerization process undergone by these compounds.

Introduction

Strained, ring-tilted [*n*]-metallocenophanes have attracted increasing interest due to their ability to function as surface derivatization agents[1] and to undergo thermally and anionically induced or transition-metal-catalyzed ring-opening polymerization (ROP) reactions.[2−17] The high-molecular-weight polymers which result contain transition metals in the main chain and exhibit a variety of interesting electrochemical, morphological, and magnetic properties. They can also serve as interesting precursors to novel ceramics.[4−6,11] This polymerization behavior seems to correlate with an increased ring tilt of the cyclopentadienyl rings, which may be taken as an indication of the ring strain present in these molecules.[18,19]

The ferrocenophanes studied are $[Fe(\eta\text{-}C_5H_4)_2SiMe_2]$ (**1**), $[Fe(\eta\text{-}C_5H_3Me)_2SiMe_2]$ (**2**), $[Fe(\eta\text{-}C_5H_4)(\eta\text{-}C_5Me_4)SiMe_2]$ (**3**), $[Fe(\eta\text{-}C_5Me_4)_2SiMe_2]$ (**4**), $[Fe(\eta\text{-}C_5H_4)_2C_2H_4]$ (**5**), and $[Fe(\eta\text{-}C_5H_4)_2S]$ (**6**) (Table 1). Values for important structural angles are given in Table 1;[4,19,20] no crystal structure data are available for **3**.

(1) Fischer, A. B.; Kinney, J. B.; Staley, R. H.; Wrighton, M. S. *J. Am. Chem. Soc.* **1979**, *101*, 6501−6506.

(2) Manners, I.; Foucher, D. A.; Tang, B. Z. *J. Am. Chem. Soc.* **1992**, *114*, 6246.

(3) Manners, I.; Finckh, W.; Tang, B. Z.; Foucher, D.; Zamble, D. B.; Ziembinski, R.; Lough, A. *Organometallics* **1993**, *12*, 823.

(4) Manners, I. *Adv. Organomet. Chem.* **1995**, *37*, 131.

(5) Manners, I. *Adv. Mater.* **1994**, *1*, 68−71 and references therein.

(6) Manners, I.; Foucher, D.; Ziembinski, R.; Petersen, R.; Pudelski, J.; Edwards, M.; Ni, Y. Z.; Massey, J.; Jaeger, C. R.; Vansco, G. J. *Macromolecules* **1994**, *27*, 3992.

(7) Hmyne, M.; Yasser, A.; Escorne, M.; Percheron-Guegan, A.; Garnier, F. *Adv. Mater.* **1994**, *6*, 564.
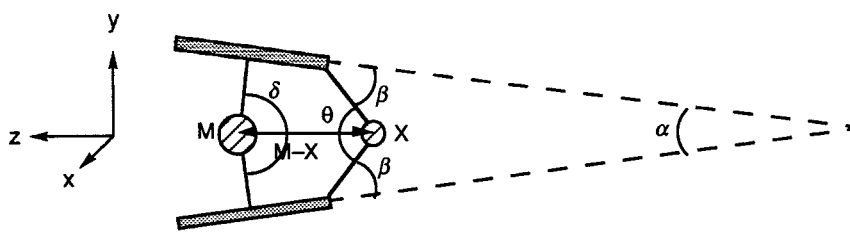
(8) Pannell, K. H.; Dementiev, V. V.; Li, H.; Cervantes-Lee, F.; Nguyen, M. T.; Diaz, A. F. *Organometallics* **1994**, *13*, 3644.
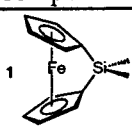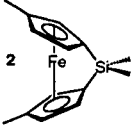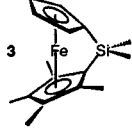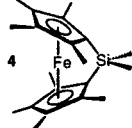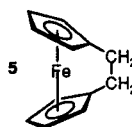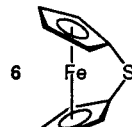
(9) Manners, I.; Pudelski, J. K.; Rulkens, R.; Foucher, D. A.; Lough, A. J.; Macdonald, P. M. *Macromolecules* **1995**, *28*, 7301.

(10) Reddy, N. P.; Yamashita, H.; Tanaka, M. *J. Chem. Soc., Chem. Commun.* **1995**, 2263.

(11) Manners, I. *Chem. Br.* **1996**, *32*(1), 46.

(12) Peckham, T. J.; Massey, J. A.; Edwards, M.; Manners, I.; Foucher, D. A. *Macromolecules* **1996**, *29*, 2396.

(13) Zechel, D. L.; Hultzsch, K. C.; Rulkens, R.; Balaishis, D.; Ni, Y. Z.; Pudelski, J. K.; Lough, A. J.; Manners, I. *Organometallics* **1996**, *15*, 1972.

(14) Barlow, S.; Rohl, A. L.; Shi, S.; Freeman, C. M.; O'Hare, D. *J. Am. Chem. Soc.* **1996**, *118*, 7578.

(15) Gómez-Elipe, P.; Macdonald, P. M.; Manners, I. *Angew. Chem., Int. Ed. Engl.* **1997**, *36*, 762.

(16) Buretea, M. A.; Tilley, T. D. *Organometallics* **1997**, *16*, 1507.

(17) O'Brien, S.; Tudor, J.; Barlow, S.; Drewitt, M. J.; Heyes, S. J.; O'Hare, D. *Chem. Commun.* **1997**, 641.

(18) Stoeckli-Evans, H.; Osborne, A. G.; Whiteley, R. H. *Helv. Chim. Acta* **1976**, *59*, 2402−2406.

(19) Manners, I.; Pudelski, J. K.; Foucher, D. A.; Honeymen, C. H.; Lough, A. J.; Barlow, S.; O'Hare, D. *Organometallics* **1995**, *14*, 2470.

Table 1. Compounds Studied and Structural Data for Compounds 1,[51] 2,[29] 4,[29] 5,[20] and 6[21]

Compound	$\alpha/°$	$\beta/°$	$\delta/°$	$\theta/°$	Fe–X/Å
1	20.8	37.0	164.7	95.7	2.690
2	18.6	39.1	166.5	96.96	2.6767
3	not available				
4	16.1	40.3	168.6	98.1	2.652
5	21.6	20.1, 12.7	164.1	n/a	n/a
6	31.1	29.0	156.9	89.0	2.795

The S-bridged compound **6** has a very large ring tilt or α value.[21] The C_2-bridged [2]ferrocenophane **5** has α and δ values similar to those for the Si-bridged [1]-ferrocenophanes though the value for β is considerably less, showing a smaller departure from planar coordination at the ring *ipso* carbon for the C_2-bridged compound.[20]

The Si-bridged [1]ferrocenophanes show a reduction in ring tilt with increased methylation of the rings (Table 1). Various reasons have been postulated for the trend of reduced tilt angle with increased methylation.[19] Methyl groups brought together at the α-positions of opposing Cp rings could lead to unfavorable steric interactions. This cannot, however, explain the reduced tilt in **2**, as the methyl groups are now at the β-position and actually move farther apart on tilting. Iron–

cyclopentadienyl bonding is strengthened by methylation.[22] With stronger Fe–ring bonding, an increasing α value leads to a relatively greater decrease in bonding energy; therefore, increasingly methylated ferroceno-phanes adopt less tilted structures.

Other structural features, as well as ring tilt, vary in a smooth way with increased methylation: (a) β, the angle between the ring plane and the *ipso*-C–Si bond, increases; (b) the *ipso* C–Si bond length increases; (c) the angle θ, *ipso*-C–Si–*ipso*-C, increases; (d) the angle between the two methyl substituents on the Si de-creases; (e) the angle δ at the Fe atom defined by the ring centroids increases; (f) the displacement of the Fe atom from the line joining the ring centroids decreases.

Thus, as the ring tilt in these species decreases with methyl substitution of the cyclopentadienyl rings, strain is manifested by increasing structural distortion about the bridging group and *ipso* carbons. The Fe–Si distance is reduced as methyl substitution increases. While this distance in all the compounds is greater than

(20) Nelson, J. M.; Nguyen, P.; Peterson, R.; Rengel, H.; Macdonald, P. M.; Lough, A. J.; Manners, I.; Raju, N. P.; Greedan, J. E.; Barlow, S.; O'Hare, D. *Chem. Eur. J.* **1997**, *3*, 573.
(21) Rulkens, R.; Gates, D. P.; Balaishis, D.; Pudelski, J. K.; McIntosh, D. F.; Lough, A. L.; Manners, I. *J. Am. Chem. Soc.* **1997**, *119*, 10976.
(22) Park, C.; Almlof, J. *J. Chem. Phys.* **1991**, *95*, 1829.

Table 2. Principal Vertical IE Features (eV) and Adiabatic First IE Values (eV) of PE Spectra of 1−6 and Oxidation Potential ($E_{1/2}$/V) versus Ferrocenium/Ferrocene (at 0.00 V) in CH_2Cl_2 with 0.1 M $[NH_4][PF_6]$[29]

band or value	1	2	3	4	5	6	ferrocene[a]	assign
adiabatic first IE	6.35	6.29	6.18	5.92	6.49	6.80	6.65	
A	6.84	6.66	6.57	6.33	6.84	7.12	6.88	metal d
	6.90	6.84	6.60		7.06	7.60	7.23	
						8.96		S p
B	8.74	8.39	8.22	7.84	8.54	9.32	8.72	ring π
	9.09	8.76			8.94		8.87	
	9.73	9.14	9.03	8.65	9.18	9.56	9.14	
					9.40		9.39	ring π
C	10.58	10.19	10.10	9.811	11.26	11.65	n/a	*ansa* bridge
		10.52	10.34	0.58		12.03		
		10.78						
$E_{1/2}$	0.00	−0.10	−0.21	−0.39	−0.01	+0.22	0.00	

[a] Reference 25.

the sum of the covalent radii and greater than representative Fe−Si bond lengths, this observation has led to the suggestion that there is a direct interaction between Fe and Si.[19]

Vondrák[23] has studied the [3]ferrocenophanes Fe-$(C_5H_4)_2(CH_2)_3$, which, by analogy with 2-Fe[C_5H_3-(CEtPhOH)](C_5H_4)(CH_2)$_3$,[24] is expected to have a ring tilt of ca. 10°, and Fe(C_5H_4CHMe)$_2$O, which may have a slightly greater ring tilt. The PES spectra resembled those of unbridged analogues such as 1,1′-dimethylferrocene[25] and 1,1′-diethylferrocene[26] but with a somewhat reduced separation between the a_1' and e_2' metal based ionizations. No evidence was found for effective removal of the degeneracy of the e_2' orbitals, but the molecules have much smaller ring tilts than the [1]ferrocenophanes of the present study. The [3]ferrocenophane Fe(C_5H_4)$_2$S$_3$, with a ring tilt of 2.85°,[27] showed a PES spectrum similar to that of the unbridged analogue Fe(C_5H_4SMe)$_2$.[28]

The aim of this study is, by using the combined techniques of photoelectron (PE) spectroscopy and density functional theory (DFT), to investigate the electronic structure of a series of [1]ferrocenophanes and the influence of the bridge on the geometry of these species.

Experimental Section

The ferrocenophanes were prepared as described previously (1,[1] 2−4,[29] 5,[20,30] 6[21,31]).

He I and He II PE spectra of 1−6 were measured using a PES Laboratories 0078 spectrometer interfaced with an Atari microprocessor which enables accumulation of a spectrum by repeated scans. Spectra were calibrated using He, Xe, and N$_2$.

Computational Details. All calculations were carried out using the Amsterdam density functional (ADF) program system, version 2.0.1.[32] For geometry optimizations and calculation of ionization and excitation energies the electronic configurations of the molecular systems were described by an uncontracted triple-ζ basis set of Slater-type orbitals (STO). Hydrogen, carbon, silicon, and sulfur were given extra polarization functions: 2p on H and 3d on C, Si, and S. The cores of the atoms were frozen: C up to 1s, Si, and S to 2p, and Fe up to 2p. For calculations of bending energy and d orbital populations on ferrocene and octamethylferrocene a more restricted basis set was used without polarization functions (double-ζ STOs for the main-group elements but triple-ζ for Fe), and the Fe core was frozen to the 3p level.

Energies were calculated using Vosko, Wilk, and Nusair's local exchange correlation potential[33] with nonlocal-exchange

corrections by Becke[34] and nonlocal correlation corrections by Perdew.[35,36] The nonlocal correction terms were utilized in calculating gradients during geometry optimizations, so as to find the nonlocal minimum.

Ionization energies (IE) were estimated by calculating energies for the molecular ions in their ground and excited states. In all cases the geometries were fixed at that found for the optimum structure for the molecule to enable comparison with the experimental vertical IE. Excitation energies for the d−d and the first charge-transfer bands of the neutral molecules 1 and 6 were calculated in a similar manner.

Results and Discussion

The low-ionization-energy (IE) regions of the He I spectra of 1−6 are presented in Figure 1. Principal IE features are given in Table 2. The higher IE region shows the normal broad IE bands associated with C−C and C−H ionizations.[37] The He II spectra show an increase in relative intensity of the first band associated with metal 3d ionizations.[38] For 6 band B decreases considerably in comparison with band B′ in the He II spectrum (Figure 2).

The spectra (Figure 1) show well-defined band regions in common with PE spectra of other metallocenes.[37,38] The region A can be identified as ionization of the six metal d electrons and region B as ionizations that are chiefly cyclopentadienyl in character. In the case of 3, where one ring is permethylated and the other is not, region B is separated into two bands: the lower IE band

(23) Vondrák, T. *Polyhedron* **1985**, *4*, 1271−1272.
(24) Lecomte, C.; Dusausoy, Y.; Protas, J.; Moïse, C.; Tirouflet, J. *Acta Crystallogr.* **1973**, *B29*, 488−493.
(25) Evans, S.; Green, M. L. H.; Jewitt, B.; Orchard, A. F.; Pygall, C. F. *J. Chem. Soc., Faraday Trans. 2* **1972**, *68*, 1847−1865.
(26) Vondrák, T. *J. Organomet. Chem.* **1986**, *306*, 89−98.
(27) Davis, B. R.; Bernal, I. *J. Cryst. Mol. Struct.* **1972**, *2*, 107−114.
(28) Vondrák, T.; Sato, M. *J. Organomet. Chem.* **1989**, *1989*, 207−215.
(29) Pudelski, J. K.; Foucher, D. A.; Honeyman, C. H.; Lough, A. J.; Manners, I.; Barlow, S.; O'Hare, D. *Organometallics* **1995**, *14*, 2470−2479.
(30) Nelson, J. M.; Rengel, H.; Manners, I. *J. Am. Chem. Soc.* **1993**, *115*, 7035−7036.
(31) Pudelski, J. K.; Gates, D. P.; Rulkens, R.; Lough, A. J.; Manners, I. *Angew. Chem., Int. Ed. Engl.* **1995**, *34*, 1506.
(32) Baerends, E. J.; te Velde, G. ADF, version 2.0.1; *Department of Theoretical Chemistry, Vrije Universiteit, Amsterdam*, 1996.
(33) Vosko, S. H.; Wilk, L.; Nusair, M. *Can. J. Phys.* **1980**, *58*, 1200.
(34) Becke, A. D. *Phys. Rev.* **1988**, *A38*, 2398.
(35) Perdew, J. P. *Phys. Rev. B* **1986**, *34*, 7046.
(36) Perdew, J. P. *Phys. Rev. B* **1986**, *33*, 8822.
(37) Green, J. C. *Struct. Bonding (Berlin)* **1981**, *43*, 37.
(38) Cauletti, C.; Green, J. C.; Kelly, M. R.; Powell, P.; van Tilborg, J.; Robbins, J.; Smart, J. *J. Electron Spectrosc. Relat. Phenom.* **1980**, *19*, 327.
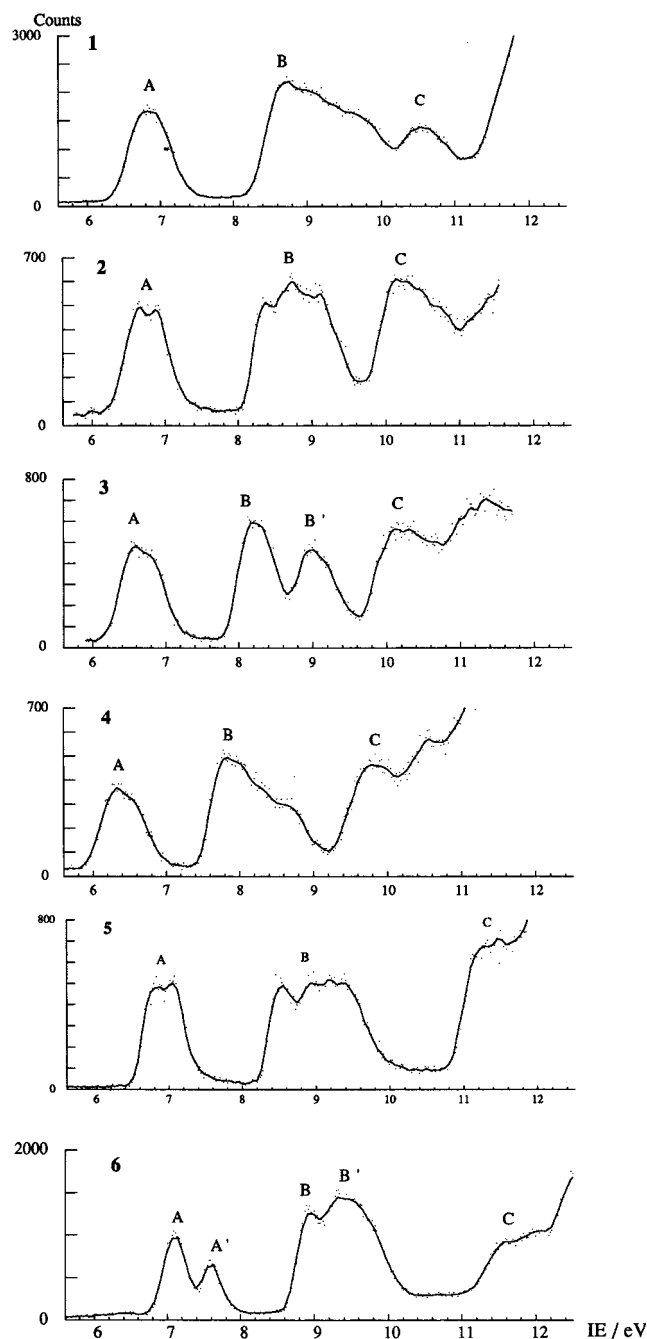
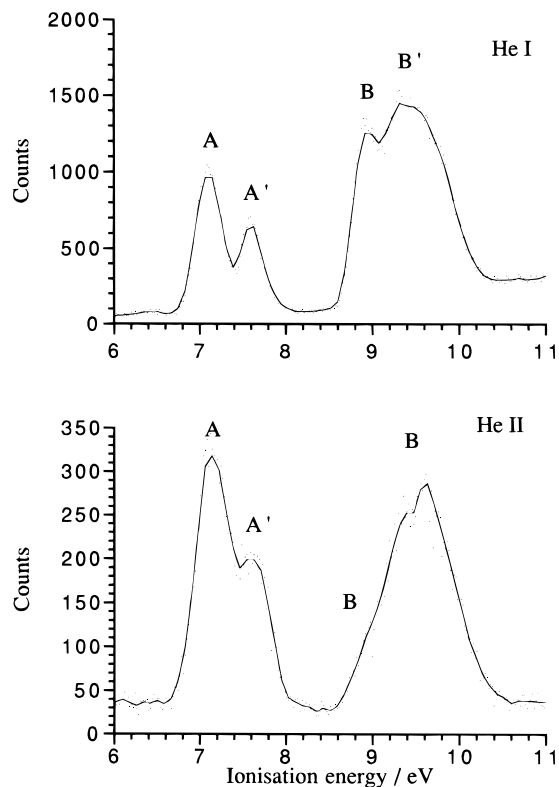**Figure 1.** He I PE spectra of **1**–**6**.

Figure 2. He I and He II PE spectra of **6**.

localized orbitals. Assignments can, therefore, be made according to Table 2.

The series show differences in d-band profile from that of ferrocene. It is well-established[41−43] that bending of a $M(\eta\text{-}C_5H_5)_2$ moiety causes the frontier orbitals to lose degeneracy and change in energy. This perturbation of the d levels is seen clearly in the PE spectra of the *ansa*-bridged metallocenes. In ferrocene the a_1 ionization occurs as a sharp band superimposed on the high-IE side of the e_2 ionization; in all of the spectra of **1**–**5** the d band is almost featureless, though in some cases two maxima may be distinguished. This is consistent with loss of degeneracy of the e_2 orbitals on bending and mixing of the d_{z^2} and $d_{x^2-y^2}$ orbitals. For **6** the d region has two distinct bands, the one with the lower IE, A, being approximately twice the intensity of the other, A′. Thus, the perturbation and mixing of the orbitals seems to have proceeded further with the greater inter-ring angle found for **6**.

A noticeable trend is the shift to lower ionization energy of the d ionizations with increased methyl substitution, as has been found previously for substituted ferrocenes.[37,38]

Comparison of the d ionizations of **1** and **5** with that of ferrocene is not straightforward. As the band shapes are broader for the *ansa*-bridged compounds, it is difficult to identify comparable features, but the center of gravity of the band seems very little shifted in **1** and **5** from that of ferrocene, despite substitution and bending. This is consistent with the electrochemistry. The oxidation potentials of **1**–**5** are shown in Table 2.

may be associated with ionization from the permethylated ring and the higher with ionization from the non-methylated ring. In the case of **6** the relatively low intensity of band B in the He II spectrum suggests that it may be due to an S-based ionization.

In addition, the silicon-bridged ferrocenophanes **1**–**4** show band C in the region 9−11 eV which is characteristic of ionization from Si−C σ bonding orbitals,[39,40] where a window of no ionization occurs for ferrocene. For **5** a band, also labeled C, occurs at higher IE which may be assigned to ionizations from the C−C bonds of the bridge. Band C for **6** is associated with S−C

(39) Evans, S.; Green, J. C.; Joachim, P. J.; Orchard, A. F.; Turner, D. W.; Maier, J. P. *J. Chem. Soc., Faraday Trans. 2* **1972**, *68*, 1161.
(40) Evans, S.; Green, J. C.; Jackson, S. E. *J. Chem. Soc., Faraday* **1973**, *69*, 191.

(41) Green, J. C.; Green, M. L. H.; Prout, C. K. *J. Chem. Soc., Chem. Commun.* **1972**, 421.
(42) Green, J. C.; Jackson, S. E.; Higginson, B. *J. Chem. Soc., Dalton Trans.* **1975**, 403.
(43) Hoffmann, R.; Lauher, J. W. *J. Am. Chem. Soc.* **1976**, *98*, 1729.

Table 3. Optimized (Experimental) Bond Lengths (Å) and Angles (deg) from the DFT Calculations for Ferrocene,[52] 1,[51] 5,[20] and 6[21,31]

	ferrocene D_{5h}	1	5	6
Fe−C	2.067 (2.064)	2.03−2.11 (1.99−2.06)	1.99−2.10 (1.97−2.07)	1.98−2.10 (1.97−2.09)
C−C ring	1.436 (1.440)	1.43−1.46 (1.40−1.46)	1.43−1.45 (1.41−1.45)	1.43−1.4 (1.42−1.45)
C−H	1.087 (1.104)	1.087	1.087	1.086
α		20.8 (20.8)	23.0 (21.6)	30.7 (31.05)
β		38.1 (37.0)		28.9 (29.0)
θ		96.6 (95.7)		88.7 (89.0)
C_{ipso}−X		1.912 (X = Si) (1.85−1.87)		1.828 (X = S) (1.81)
C−X		1.891 (Si−Me) (1.83−1.86)		
C−C_{ipso}			1.531 (1.54)	
C−C			1.558 (1.54)	
C−C−C_{ipso}			110.2 (1095.9)	
Fe···X		2.718 (X = Si) (2.690)	2.898 (X = C)	2.816 (X = S) 2.80

Table 4. Comparison of Theoretical (Experimental) IE Values (eV) for Ferrocene, 1, 5, and 6

orbital	ferrocene	orbital	1	orbital	5	orbital	6
e_2'	7.12 (6.88)	$3b_1$	6.85 (6.84)	3b	6.82 (6.84)	$3b_1$	7.11 (7.12)
a_1'	7.18 (7.23)	$4a_1$	6.89 (6.84)	4a	a (6.84)	$4a_1$	7.18 (7.12)
		$3a_1$	7.17 (6.84)	3a	7.09 (7.06)	$3a_1$	7.68 (7.60)
						$2b_1$	8.61 (8.96)
e_1'	8.59 (8.72)	$2a_1$	8.39 (8.74)	2a	8.31 (8.54)	$2a_1$	9.04 (9.32)
		$2b_1$	8.65 (8.74)	2b	8.68 (8.94)	$1b_1$	9.21 (9.32)
e_1''	9.22 (9.14)	$2b_2$	9.16 (9.09)	1a	9.16 (9.18)	$2b_2$	9.59 (9.56)
		$1a_2$	9.18 (9.09)	1b	9.32 (9.40)	$1a_2$	9.59 (9.56)
		$1a_1$	9.92 (9.73)			$1a_1$	11.05 (11.65)
		$1b_2$	9.93 (9.73)			$1b_2$	11.55 (12.03)
		$1b_1$	10.14 (9.73)				

^{a} SCF convergence was not achieved for this configuration.

These show a decrease in oxidation potential on methylation which correlates well with the decrease in adiabatic IE (Table 2). Also **1** has an $E_{1/2}$ value identical with that of ferrocene itself, and that for **5** is only shifted by −0.01 V. Compound **6** has a greater adiabatic IE than is found for ferrocene, and its $E_{1/2}$ value is 0.2 V more positive than that of ferrocene.[21]

DFT Calculations. The initial aim of the calculations was to see whether the ground-state structures and ionization energies could be modeled with a reasonable degree of accuracy by density functional methods.

The level of calculation chosen for these tasks was that which gave the best agreement with the experimental data for ferrocene. The Fe 3s and 3p electrons were unfrozen and were included in the basis set, and gradient corrections were employed throughout the geometric optimization procedure. The molecular symmetry was constrained to C_{2v} for **1** and **6** and to C_2 for **5**. The predicted geometries are compared with the experimental values for ferrocene, **1**, **5**, and **6** in Table 3.

Agreement betwen calculated and experimental structural parameters is, on the whole, highly satisfactory. Particularly impressive is the good agreement in the values for α and θ.

A comparison of calculated and experimental vertical IE values is given in Table 4. Here comparison is hampered by the fact that many of the spectral bands are broad and overlapping, making the experimental vertical IE difficult to define. Nevertheless, within this limitation, theory and experiment are seen to be close in their numerical predictions and the assignments

indicated in Table 2 are vindicated. Of particular note is the separation found for the d bands for **6**, which fits the model of increased separation of the two a_1 orbitals with increasing α. Also, examination of the orbitals confirms that the band B, which correlates with the $2b_1$ ionization, is due to ionization from the nonbonding S p orbital.

UV−Vis Spectroscopy. The visual appearance of the bridged ferrocenophanes is particularly striking in that, while ferrocene has an orange hue, **1** is red and **6** is purple. The UV−vis spectra of **1−6** have been recorded[29] and the bands assigned by comparison with the electronic spectrum of ferrocene.[44] The first spin-allowed bands for **1** and **2** are more intense and are at a longer wavelength than that of ferrocene (band II). Lowering symmetry from D_{5d} to C_{2v} results in the splitting of both the filled e_{2g} orbitals, which become a_1 and b_1 in symmetry, and also the empty e_{1g} orbitals, which become b_2 and a_2 in symmetry. Inspection of unoccupied orbitals shows the lowest unoccupied MO (LUMO) and second unoccupied MO (SUMO) of **1** and **6** to be derived from the e_{1g} MO of ferrocene. Calculations of the wavelengths for nine possible d−d transitions of **1** and **6** are given in Table 5. Agreement with the position of the first spin-allowed bands of **1** and **6** is good. That of **1** is spread from 575 to *ca.* 390 nm with a maximum at 482 nm; that of **6** has a wider spread (correlating with the wider spread of d band IE) from 600 to 380 nm and a lower energy maximum of 504 nm. These features are reproduced by the calculations.

(44) Sohn, Y. S.; Hendrickson, D. N.; Gray, H. B. *J. Am. Chem. Soc.* **1971**, *93*, 3603−3612 and references therein.
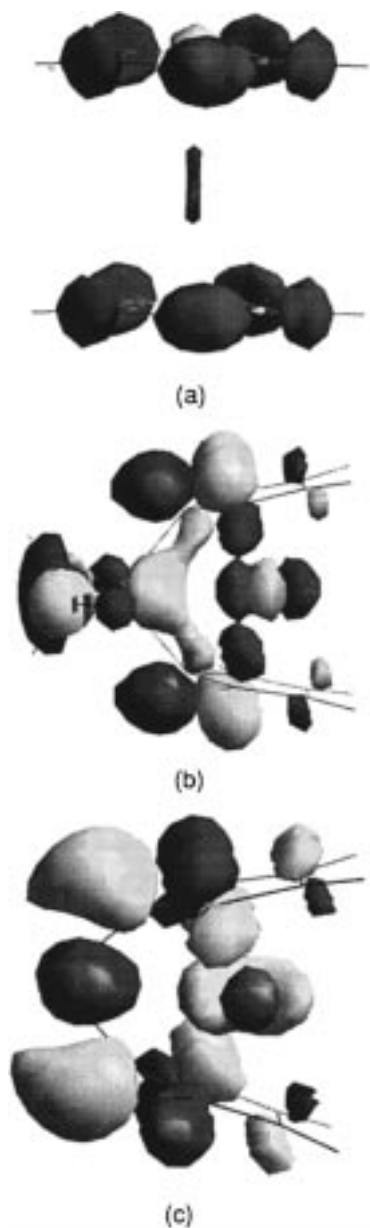
Figure 3. Representation of the third unoccupied orbital of (a) ferrocene, (b) **1**, and (c) **6**.

Table 5.　Calculated Transition Wavelengths (nm) for 1 and 6

transition type	transition	1	6
d−d	$3b_2 \leftarrow 4a_1$	561	574
	$3b_2 \leftarrow 3b_1$	495	504
	$2a_2 \leftarrow 4a_1$	517	501
	$2a_2 \leftarrow 3b_1$	493	499
	$2a_2 \leftarrow 3a_1$	452	442
	$3b_2 \leftarrow 3a_1$	424	400
d−ligand	$5a_1 \leftarrow 3b_1$	315	363
	$5a_1 \leftarrow 4a_1$	298	343
	$5a_1 \leftarrow 4a_1$	282	303

The third unoccupied orbital in these two bridged ferrocenophanes is significantly lowered in energy and is spatially different from that of ferrocene. Representations of the third unoccupied orbital, a_1 in symmetry, in the three compounds are given in Figure 3. In Table 5 the wavelengths for excitations from the three d orbitals to the third unoccupied orbital are also given. These are in good agreement with the experimental position of the second band systems of **1** and **6**, which

Table 6.　Mulliken Population Analysis of the d Orbital Occupancy of Ferrocene, 1, and Ferro-20[a]

	z^2 (a₁)	$x^2 - y^2$ (a₁)	xy (a₂)	xz (b₁)	yz (b₂)
ferrocene	1.73	1.86	0.89	1.66	0.89
Ferro-20	1.71	1.85	0.89	1.66	0.90
1	1.68	1.84	0.90	1.69	0.91

[a] For all compounds, including ferrocene, the coordinate system is that of Figure 2 with the z axis as the C_2 axis passing through the Fe and bisecting the bridge.

have maxima at 300 and 322 nm, respectively. However, such a simple assignment of the visible spectrum should be viewed with caution. In ferrocene itself, the second spin-allowed band system, band III, which has a maximum at 325 nm, is assigned to a d−d transition.[44] It is possible that this band has also moved to longer wavelength in the ferrocenophanes and is now part of the first broad band, as the calculations suggest. It may also be the case that DFT is failing to reproduce the correlation in the excited states and the second band in the ferrocenophanes is also essentially a d−d transition.

The third unoccupied orbital is of particular interest in the context of the chemistry of **1** and **6**. It has a large contibution from the *ipso* carbons of the rings and is antibonding between the *ipso* carbons and the bridge. This makes it a very attractive candidate for the site of nucleophilic attack in the ring-opening polymerization reactions undergone by these ferrocenophanes.

Mössbauer Spectroscopy. Ferrocenophanes have been shown to have quadrupolar splittings (ΔE_q) substantially different from those of the unbridged analogues.[29,45,46] To date, interpretation of this Mössbauer parameter, which is a measure of the electric field gradient at the Fe nucleus, has been qualitative and has been discussed in terms of the relative populations of the Fe d orbitals.[47] In an axially symmetric ferrocene, ΔE_q is decreased by occupation of the $x^2 - y^2$ and xy orbitals and increased by population of the xz and yz orbitals; the effect of population of the former e₂ orbitals is twice as great as that of occupation of the latter e₁ orbitals. The small values of the Si-bridged ferrocenophanes relative to the unbridged analogues have been taken as an indication of depletion of electron density in the e₂ set of d orbitals and interpreted as providing evidence for direct donation of electron density into Si 3d orbitals.[29,48,49] This, together with the Fe−Si distances found in these compounds, has led to the proposal for an Fe−Si bond (albeit a weak one).[29,49] A key piece of evidence that supports an Fe−Si interaction is the report that the C_2-bridged species [Fe(η-C₅H₄)₂C₂-Me₄] has a ΔE_q value close to that of ferrocene, even though the tilt angle (ca. 21°) is close to that of **1**.

Evaluation of quadrupolar splittings is computationally very demanding and is outside the scope of our work reported here. However, such calculations as we have performed give us an opportunity to test the variation of d electron population on bending a ferrocene and on

(45) Good, M. L.; Buttone, J.; Foyt, D. *Ann. N.Y. Acad. Sci.* **1974**, *239*, 193.
(46) Miller, J. S.; Glatzhofer, D. T.; O'Hare, D.; Reiff, W. M.; Chakraborty, A.; Epstein, A. J. *Inorg. Chem.* **1989**, *28*, 2930.
(47) Houlton, A.; Miller, J. R.; Roberts, R. M. G.; Silver, J. *J. Chem. Soc., Dalton Trans.* **1990**, 2181 and references therein.
(48) Clemance, M.; Roberts, R. M. G.; Silver, J. *J. Organomet. Chem.* **1983**, *243*, 461.
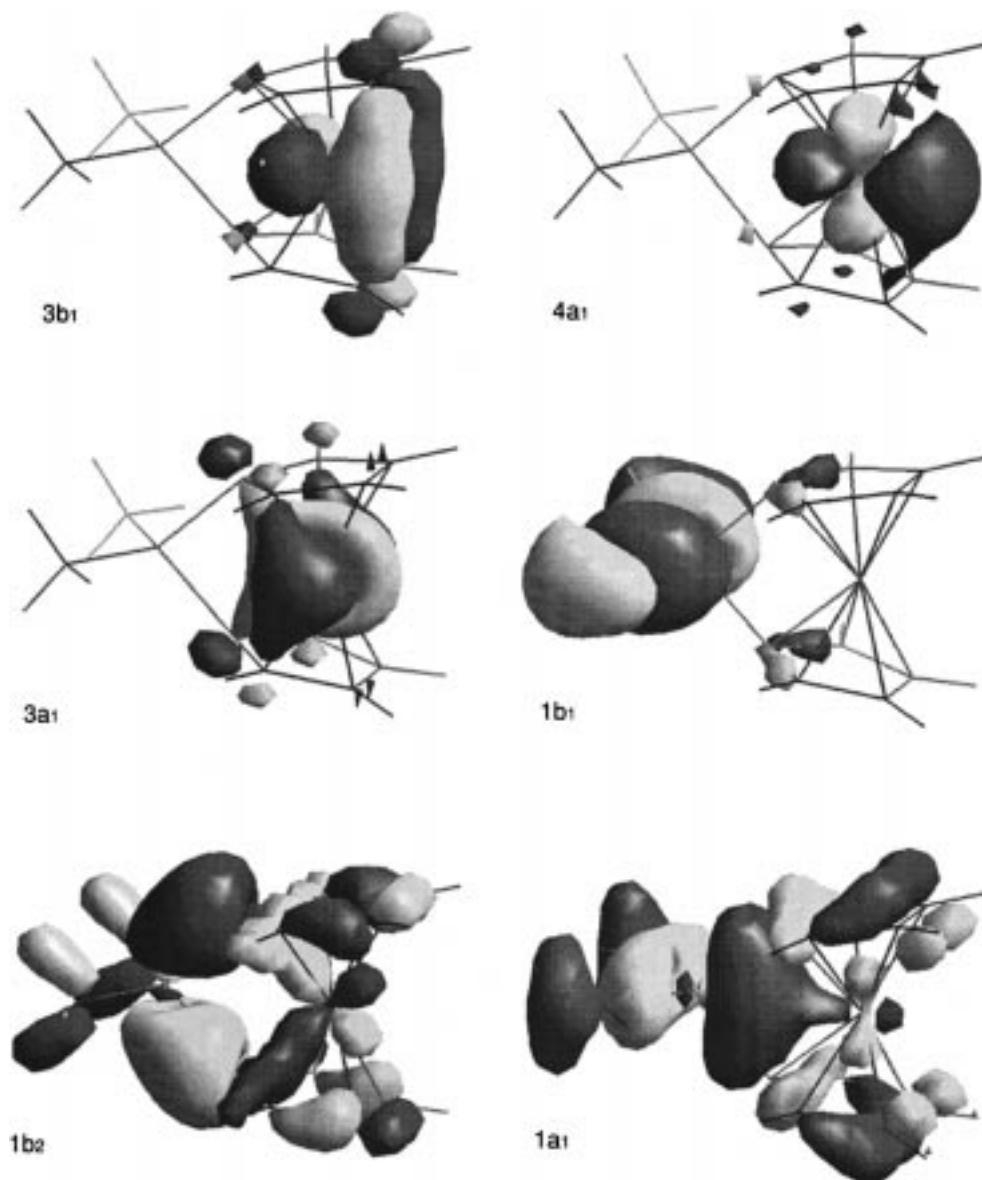(49) Silver, J. *J. Chem. Soc., Dalton Trans.* **1990**, 3513.

Figure 4. Representations of selected orbitals for **1**.

linking the rings with bridging atoms. A Mulliken population analysis of the occupation of the Fe d orbitals in ferrocene with inter-ring angles of 0 and 20° (Ferro-20) and for **1** is given in Table 6. The coordinate system for ferrocene, with its rings parallel, is taken, unconventionally, with the y axis as the 5-fold symmetry axis, to facilitate direct comparison between ferrocene and the other compounds, which with C_{2v} symmetry have the z axis as the 2-fold rotational axis.

Very little variation is found on bending or on bridge formation. Given the vagaries of Mulliken population analyses, it would be unwise to read anything into the very small changes found. It thus seems unlikely that changes in the d-orbital population can account for the variations found for the electric field gradient at the Fe nucleus, and any inference that is drawn as to direct Fe–Si bonding seems not to be justified by this analysis.

It is also noteworthy that there is little difference between the orbital populations of **1**, which has an inter-ring angle close to 20°, and ferrocene, with the rings at 20°. Both **1** and Ferro-20 are calculated to have small dipole moments: 0.114 and 0.617 D, respectively.

Whether this contributes to the change in quadrupole splitting must be considered.[49,50]

Orbital Structure. The ability of DFT to match both structural and electronic experimental parameters for these compounds gives us confidence in examining the electronic structure in more detail; in particular, we are looking for any direct interaction between Fe and the bridging atom.

In this context representations of selected one-electron wave functions of **1** are shown in Figure 4. The top three occupied orbitals, $3b_1$, $4a_1$, and $3a_1$, are largely d in character and show no visible Si contribution. The lower lying orbitals $1b_2$ and $1a_1$, which bind the Si to the *ipso* carbons, do show a d contribution from the Fe. However, the interaction is multicentered, in particular with the carbon atoms of the ring, rather than with the

(50) Trautwein, A.; Reschke, R. d. I.; Harris, F. E. *J. Phys., Colloq.* **1976**, *37*, C6–463.

(51) Finckh, W.; Tang, B.-Z.; Foucher, D. A.; Zamble, D. B.; Ziembinski, R.; Lough, A. J.; Manners, I. *Organometallics* **1993**, *12*, 823–829.

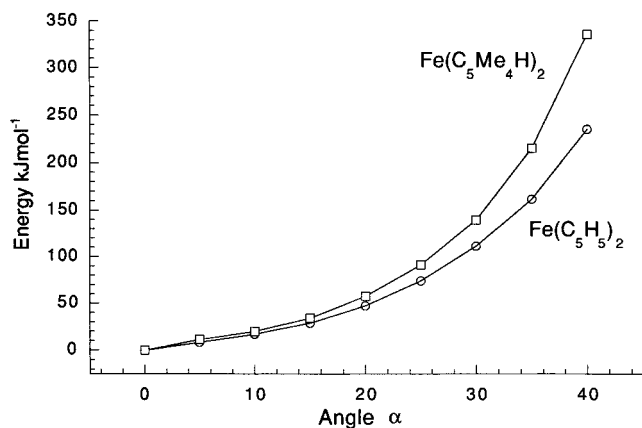(52) Haaland, A. *Acc. Chem. Res.* **1979**, *12*, 415.

Figure 5. Plot showing the variation in energy of ferrocene and octamethylferrocene as a function of ring centroid–Fe–ring centroid angle.

silicon directly. Mulliken analysis gives a value of 0.00 for the Fe–Si overlap population.

Bending Strain. To investigate the strain involved in bending a metallocene, we calculated the energy of ferrocene and octamethylferrocene as a function of inter-ring angle. The other geometric parameters were kept fixed at the optimized values for the parallel ring structure. In the case of octamethylferrocene the direction of the bend made the ring carbons bearing hydrogen approach each other. The results are shown in Figure 5, where the energies of the two compounds are plotted as a function of α. It is evident that the methylated ferrocene requires more energy to distort than ferrocene itself. For example, bending to an α value of 20° requires around 10 kJ mol^{-1} more energy for octamethylferrocene than for ferrocene. Bending ferrocene to an

α value of 30° as is found for **6** requires over 100 kJ mol^{-1}, which is a reasonable proportion of the value found for the strain energy of **6** determined by differential scanning calorimetry (130 ($\pm$20) kJ mol^{-1}).[21]

Conclusions

Photoelectron spectroscopy on the bridged ferrocenophanes **1**–**6** shows evidence for perturbation of the d-orbital structure on bending. However, ring substitution has a greater effect on the first IE than distortion of the metallocene unit from a parallel geometry. The variation in first IE along the series is in close agreement with the variation in electrochemical potential.

Density functional calculations on **1**, **5**, and **6** gave molecular geometries in excellent agreement with X-ray diffraction data. Calculations of IE were also in close agreement with experiment and confirmed the empirical assignments of the ionizations associated with the bridging atoms.

The energy needed to bend octamethylferrocene was calculated to be significantly greater than that required to bend ferrocene, as had been inferred from the structural parameters found for **1** and **4**. The energy of bending ferrocene to an α value of 30° was estimated as 100 kJ mol^{-1}, an order of magnitude similar to that for the strain energy found experimentally for **6**, which has an α value of 31°.

Estimations of excitation energies for **1** and **6** reproduced the experimental trend. The ferrocenophanes had an additional low-lying empty orbital with significant localization on the *ipso* carbons. This is proposed as a possible site for nucleophilic attack in the polymerization reaction of these compounds.